Materials Research Express

PAPER • OPEN ACCESS

Adsorption potential of macroporous Amberlyst-15 for Cd(II) removal from aqueous solutions

Materials Research Express

PAPER

Adsorption potential of macroporous Amberlyst-15 for Cd(II) removal from aqueous solutions

Rabil Razzaq[1], **Khizar Hussain Shah**[2,5], **Muhammad Fahad**[3,5], **Abdul Naeem**[4] and **Tauqir A Sherazi**[2]

[1] Environmental and Energy Engineering Sciences, University of Udine, 33100 Udine, Italy
[2] Department of Chemistry, COMSATS University Islamabad, Abbottabad Campus, University Road 22060, Abbottabad, Pakistan
[3] Department of Electrical and Computer Engineering, COMSATS University Islamabad, Abbottabad Campus, University Road 22060, Abbottabad, Pakistan
[4] National Centre of Excellence in Physical Chemistry, University of Peshawar, Peshawar 25120, Pakistan
[5] Authors to whom any correspondence should be addressed.

E-mail: khizarshah@cuiatd.edu.pk **and** drmuhammadfahad@gmail.com

Keywords: adsorption, amberlyst-15, langmuir and D-R models, thermodynamic parameters

OPEN ACCESS

RECEIVED
25 October 2019

REVISED
18 January 2020

ACCEPTED FOR PUBLICATION
22 January 2020

PUBLISHED
10 February 2020

Abstract

The macroporous ion exchange resins are unique and most suitable for the adsorption of heavy metal ions due to their porous three-dimensional structures and large specific surface areas. In the current investigation, a macroporous sulphonic acid cation exchange resin Amberlyst-15 was implemented for the adsorption of Cd (II) using batch adsorption technique to evaluate its removal efficiency. The characterization of resin surface was performed by several techniques: Scanning Electron Microscopy/Energy dispersive x-ray Spectroscopy (SEM/EDS), Thermogravimetric analysis (TGA), Fourier-transform infrared spectroscopy (FT-IR), Brunauer–Emmett–Teller (BET) surface area and Point of zero charge (PZC). The effects of various experimental parameters such as time, temperature, concentration, pH and dosage amount were examined in detail. The optimum pH for maximum uptake of Cd(II) onto the Amberlyst.15 was observed at pH 3 showing the efficient working of resin under highly acidic conditions. The results also proved that Amberlyst-15 showed tremendous adsorption potential toward Cd(II) removal; 99.95% removal within 30 min reaction time and 2.01 mmol g^{-1} maximum adsorption capacity at 323 K. The adsorption data was well described by Langmuir adsorption isotherm and pseudo second order models. The thermodynamic parameters revealed that the adsorption was endothermic, spontaneous and feasible process with increased randomness at resin surface. The free energy of adsorption (E) (13–15 kJ mol^{-1}) determined from Dubinin-Radushkevitch (D-R) model proved the ion exchange reaction mechanism for Cd(II) adsorption. The experimental results reported herein validate that Amberlyst.15 resin is a promising adsorbent for the enhanced removal of Cd(II) and other toxic metals from contaminated water and waste effluents.

1. Introduction

Nowadays, water pollution is one of the important environmental issues which arise due to the uncontrolled and untreated discharge of industrial effluents containing heavy metals and organic dyes into the ecosystem [1]. The heavy metal ions are highly stable and non-biodegradable in nature, that's why cannot be removed from water and soil easily [2]. Humans exposure to heavy metals mainly by inhalation, food and drinking water can cause many health hazards which include hypertension, damaging of lungs and liver, kidney failure, muscles pain, high blood pressure, permanent head damage, diarrhea, heartburn, food allergies, gastrointestinal infection, immature growth and abnormal development [3, 4]. Therefore, the removal of heavy metal ions from aqueous solutions becomes compulsory and challenging owing to their acute toxic effects. Many conventional techniques are available for removal of heavy metal ions which includes solvent extraction, precipitation, photocatalyrtic degradation, coagulation, reverse osmosis, membrane separation, biological degradation, ion exchange and

adsorption [5–7]. Among all these described techniques, ion exchange is most promising and versatile because of numerous advantages such as high removal efficiency, more selectively, easy operation and designing, regeneration and recovery of both adsorbate and adsorbent, no sludge formation and production of secondary pollutants. Several works have been performed on synthesis and application of different types of ion exchangers; including inorganic, organic, hybrid, and surfactant and nanoparticles supported exchangers for the removal of heavy metal ions from water and wastewater solutions [4, 8–10].

Further, in ion exchange technology, organic ion exchange resins have been considered as suitable adsorbents due to their fast reaction rate, excellent exchange capacity, easy separation and regeneration of adsorbent, high removal efficiency even at low concentration and environment friendly nature [11, 12]. Among these organic ion exchange resins, macroporous class of reins is unique due to their exceptionally high specific surface areas and more active sites, and their application for the removal of toxic metals has proved to be a great advancement in the field of ion exchange technology. They are gaining recently more interest in many environmental applications due to their greater thermal stability, more resistance to oxidation and osmotic shocks. For that reason, macroporus ion exchange resins have been extensively practiced for the adsorption of heavy metal ions, and results have shown the outstanding performance of macroporous resins D113, D151, D152, D155, NKC-9 and D72 for the removal of Dy(III), Gd(III), Ce(III), Pr(III), Co(II), Ni(II) and Pb(II) ions from aqueous solutions [13–22]. In this vicinity, some reports are also available which proved that macroporous resins have also shown better performance than gel structure or microporus type of resins because they offer comparatively faster kinetics, higher adsorption capacity and better mechanical stability [23, 24].

Amberlyst-15, one of the earliest synthesized macroporous cation exchange resin, in the past, was mostly utilized as a heterogeneous catalyst in the synthesis of many organic compounds [25]. However, it is also compulsory to have a sound knowledge and detailed investigation to determine the true potential of this resin for the adsorption of heavy metal ions. In our previous investigations, we investigated its potential for the adsorption of Cr(III) independently and in mixed metal system, and results showed tremendous performance of the resin [26]. Cd(II) is one of the heavy metal ions that can cause negative impacts on human health and environment when its concentration exceeds than the recommended limit (0.003 $mg.l^{-1}$) in surface and ground water. Therefore, its removal from aqueous solutions is compulsory to protect the environment and life on the planet [27, 28].

In the current research, the adsorption potential of Amberlyst.15 for Cd(II) was investigated under the effect of reaction time, concentration, temperature, resin dosage and pH in order to optimize the adsorption efficiency of resin. The present study will provide a theoretical base and in-depth knowledge for the successful removal of Cd(II) from aqueous solutions through ion exchange technology.

2. Materials and methods

Amberlyst-15, $CdCl_2.6H_2O$, NaOH, HCl, $NaNO_3$were obtained from BDH company (UK). All the glassware were washed thoroughly with HNO_3 (10%) and finally rinsed with distilled water prior to utilization. For stalk solution, an appropriate amount of $CdCl_2.6H_2O$ was dissolved in 1 L of doubly distilled water and then working solutions of various concentrations were prepared by simple dilution method. The calibration of pH meter was made by using buffer solutions of pH 2 and 12 before performing the adsorption experiments. The pH adjustment of solutions was done by using dilute solutions of NaOH and HCl.

2.1. Characterization of resin

Surface area analyzer (Quanta chrome NOVA 2200e, USA) was used for the calculation of surface area of amberlyst-15. For degassing purpose, sample was initially heated at 125 °C for 1 h and then analyzed for determination of surface area. The surface area and pore size distribution (PSD) were calculated by employing Brunauer–Emmett–Teller (BET) and Barrett–Joyner–Halenda (BJH) models. The surface morphology of the sample was investigated using scanning electron microscope (JEOL JSM 5910 SEM, Japan) and semi-quantitative analysis was performed using energy dispersive x-ray spectroscopy (INCA200 EDS, UK) coupled with SEM. The secondary electron SEM images (SEI) of amberlyst-15 were taken before and after the adsorption of Cd(II). FTIR analysis was carried out for the determination of vibrational frequency changes in functional groups of adsorbents before and after the adsorption of Cd(II) using a Perkin Elmer Spectrum Two model spectrometer. The spectrometer equipped with a $LiTaO_3$ detector coexists with a standard optical system to collect data in the 8300–350 cm^{-1} spectral range at a best resolution of 0.5 cm^{-1}. Prior to the analysis, samples were prepared by mixing with KBr in the 1:3 ratio and spectra was recorded in the range 4000–400 cm^{-1}. Thermogravimetric analyzer (Perkin Elmer, USA) was used to elucidate the physiochemical characteristics of the resin. The point of zero charge (PZC) was determined by well-known salt addition method [29].

2.2. Adsorption experiments

To study the contact time, 520 mg l^{-1} of Cd(II) solution was taken in a double walled glass cell and pH was maintained at 3. Then predetermined adsorbent dosage (0.1 g) was poured into the solution at constant stirring with an agitation speed of 120 rpm. A series of samples were extracted from the reaction mixture with different time intervals ranging from 1 to 120 min at different temperatures 293, 303 and 313 K. For dosage study, dose range was from 0.1 to 5 g at 293 K while keeping the other parameters constant. For pH study, temperature was kept constant at 293 K, and pH was adjusted in the range of 3–5 using concentration range of 2.68 to 1480 mg l^{-1} and adsorbent dosage of 0.5 g. To investigate the temperature and concentration effect, initial concentration of Cd(II) was ranged from 2.68 to 1480 mg l^{-1} with pH 3 and 0.5 g of dosage at 293–323 K. A temperature-controlled water shaker bath was used for constant stirring of the samples with an agitation speed of 120 rpm for 2 h. After filtration, filtered suspensions were analyzed by atomic absorption spectrometry (AAS 700 Perkin Elmer, USA) to determine Cd(II) ions concentration. All the experiments were conducted in triplicate and the results were obtained from their mean values. The following equation was employed to determine the amount of metal adsorbed per unite mass of adsorbent:

$$q_e = \frac{V_L(C_o - C_e)}{1000m} \tag{2}$$

where C_o and C_e represents the concentrations at initial and equilibrium respectively, (mol/l) for Cd(II) ions, and m is the adsorbent mass in gram where as V_L correspond to volume of metal ions solution.

3. Results and discussion

3.1. Characterization of amberlyst-15

3.1.1. Surface area and porosity

The surface area and pore size distribution of macroporous resin Amberlyst.15 were calculated under N_2 gas adsorption/desorption isotherm at 77 K. The BET surface area of the adsorbent was estimated as 105.67 m^2 g^{-1} with an average pore volume of 0.55 cc/g [30]. Similarly, from the plot for pore size distribution (figure 1(a)), it was found that large numbers of particles have a pore diameter $\geqslant$10 nm.

3.1.2. Thermogravimetric analysis

Variable weight losses were observed to occur at different temperature from the thermogravimetric analysis for Amberlyst-15 (figure 1(b)). The first 19% weight loss was noted at ~120 °C may be due to the dehydration of physically adsorbed water in the matrix. Similarly, 8% weight loss detected in 200 °C–300 °C temperature range can be attributed to the exclusion of interstitial water. Another weight loss in temperature range of 400 °C–600 °C was 23% which can be attributed to Amberlyst-15 decomposition at high temperatures [31].

3.1.3. PZC determination

The PZC is an important tool in optimizing the experimental conditions in adsorption and plays a vital role in characterization of adsorbent. This describes the pH at which the electrical charge density on the surface of adsorbent becomes zero. When pH is lower than PZC, then cations adsorption will be favored due to the positively charged surface. Conversely, when pH is greater than PZC, it will suit the anions adsorption due to negatively charged surface [32]. The Amberlyst-15 PZC was estimated using salt addition method as proposed elsewhere [33]. A plot of ΔpH (pH_i–pH_f) *versus* pH_i is mentioned in figure 1(c) which clearly shows the PZC of Amberlyst-15 at pH 2 where $\Delta pH = 0$. This value of PZC estimated in the present investigation agrees well with the values reported in literature [34, 35].

3.1.4. Surface morphology

The surface morphology of Amberlyst-15 adsorbent in pure form and after metal ions Cd(II) adsorption was investigated using SEM-EDS and results are shown in figures 2(a) and (b). Amberlyst-15 particles were not observed to possess a uniform size and most of them were seen to be cracked on their surface which can contribute to the enhancement of adsorption process.

Furthermore, it is clear from the SEM images that average particle size of the adsorbent beads was ranging from 0.5 to 0.8 mm in diameter. The corresponding EDS spectra of Amberlyst-15 before and after the adsorption of Cd(II) is shown in figure 5. It can be seen from EDS spectra of figure 3(a) that pure Amberlyt-15 contains only C, S and O which are the core elements of the resin; however, after the Cd adsorption new peaks appeared due to the adsorption of cadmium on the surface(figure 3(b)).

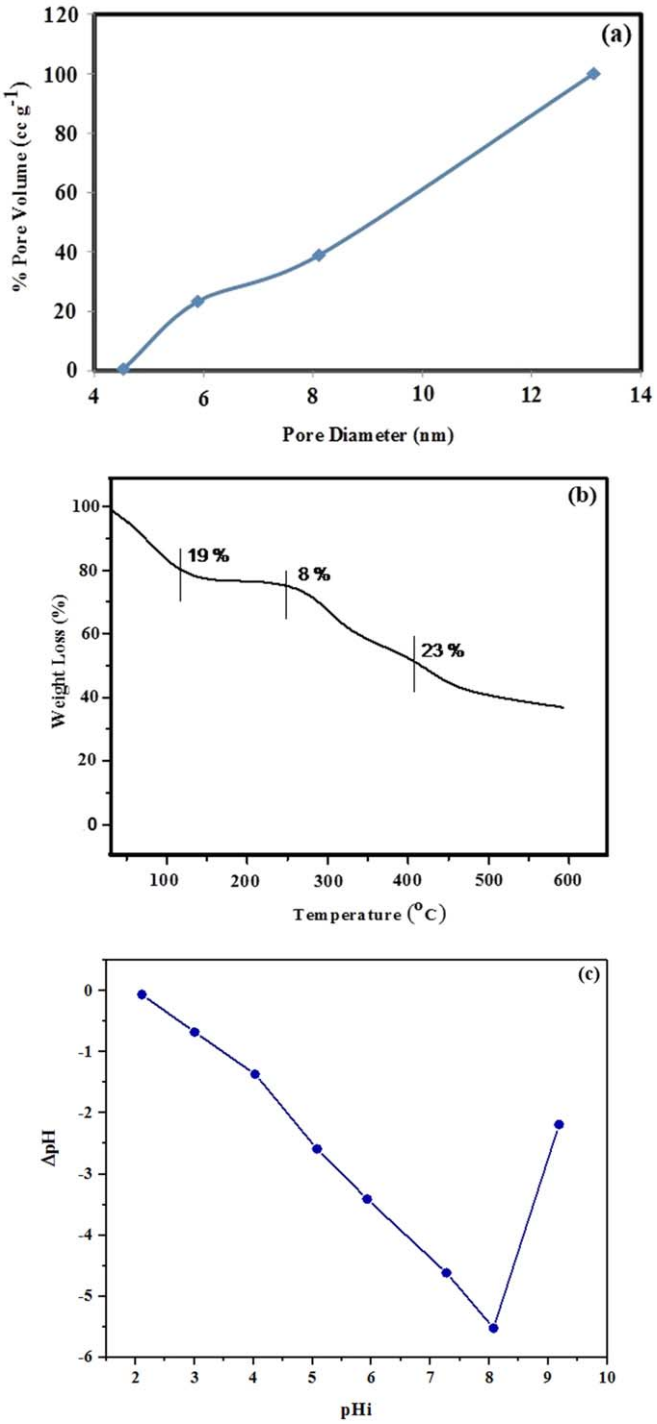

Figure 1. (a) Pore size distribution of Amberlyst-15, (b) TGA of Amberlyst-15, (c) Point of zero charge (pzc) of Amberlyst-15.

3.1.5. FTIR analysis

Figure 4 shows FTIR spectra of the samples before and after Cd(II) adsorption. It can be observed from figure 4(a) that IR spectra of Amberlyst-15 consists of numerous peaks suggesting a multi-functional structure of the resin. A broad peak and weak peak observed at 3410 and 2928 cm^{-1} is assignable to the O–H and C–H stretching vibrations, respectively [36, 37]. The bands observed at 1650 and 1500 cm^{-1} belongs to stretching vibrations of PS and DVB aromatic rings in Amberlyst-15 and two bands at 1011 and 1147 cm^{-1} may be assigned to C–C bond and to SO_3^- group stretching vibrations, respectively. Similarly, other peaks appeared less than 1000 cm^- can be assigned to SO_3^- functional site in Amberlyst-15 responsible of ion exchange reaction [38].

The intensities and position of various bands were also observed to change significantly (figure 4(b), for example, in case of pure Amberlyst, the band at 3410 cm^{-1} becomes more intense and also shifts to 3373 cm^{-1}after the adsorption which suggested the exchange of Cd(II) with H^+ ions. Similarly, the peaks at1650

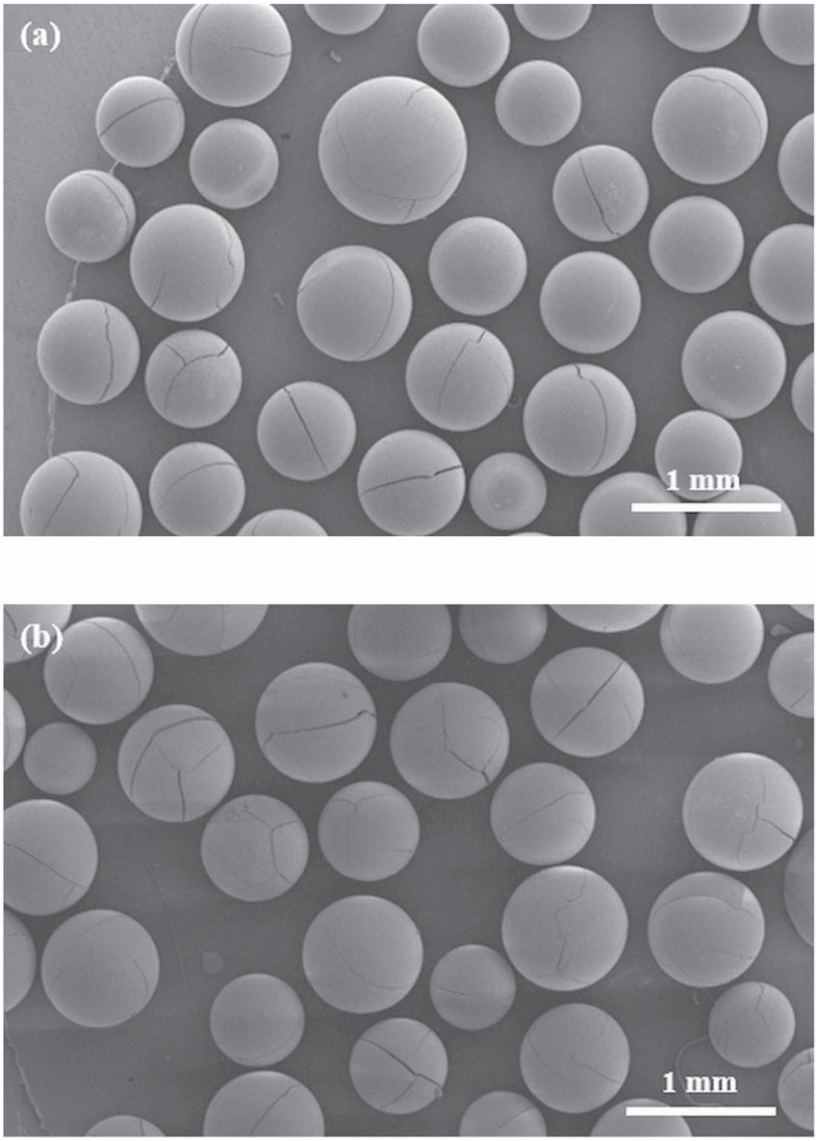

Figure 2. Secondary electron SEM images of Amberlyst-15: (a) before, and (b) after the adsorption of Cd(II)at 303 K and pH 5.

and 1147 cm^{-1} after Cd(II) adsorption shift to 1645 and 1163 cm^{-1}, respectively which can be attributed to the Cd(II) ions attachment at SO_3^- active sites.

3.2. Adsorption of Cd(II) on Amberlyst-15

3.2.1. Effect of time and temperature

The kinetic studies of metal ions adsorption onto Amberlyst-15 were investigated at pH 5 and temperature range of 293–313 K. The equilibrium data is graphically shown in figure 5.

It shows the endothermic nature of adsorption process. It is obvious from the figure that initially the rate of adsorption is very fast due to the quick transportation of metal ions from solution phase to the solid phase. This behavior is probably the result of extensive availability of binding sites on adsorbent surface, which drives fast diffusion of Cd(II) ions among the particles of resin in the beginning of reaction [39]. However, after some time, the rate decreases gradually due to the occupation of active sites and attains equilibrium in 60 and 30 min at 293 and 313 K respectively. As evident from the figure, a negligible effect of temperature was observed for Cd(II) uptake at 293 and 303 K, however, the effect of temperature was significant at 313 K. Similar behavior of temperature effect on Cd(II) adsorption was also observed elsewhere [40, 41].

3.2.2. Application of kinetic models

The kinetic studies of ion exchange adsorption are necessary to develop and design an ion exchange system for treatment of contaminated water on pilot and industrial scale [2]. The adsorption kinetic data for Cd(II) onto Amberlyst-15 were analyzed by pseudo-first order, pseudo-second order models [5, 42]. The linear form of

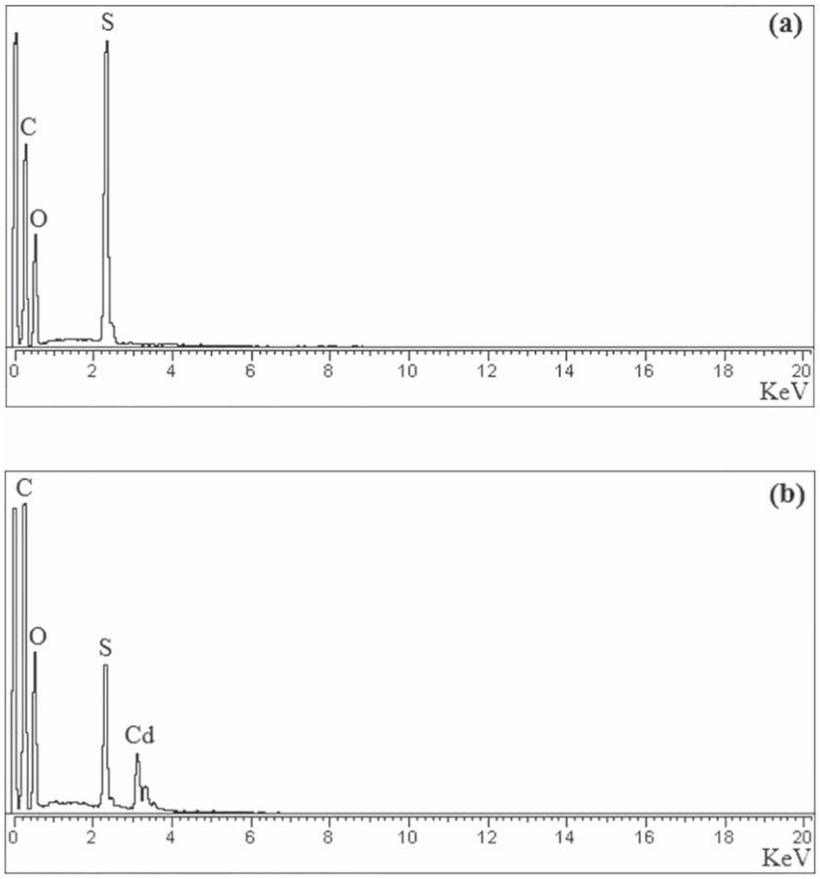

Figure 3. EDS images of Amberlyst-15: (a) before, and (b) after the adsorption of Cd(II) at 303 K and pH 5.

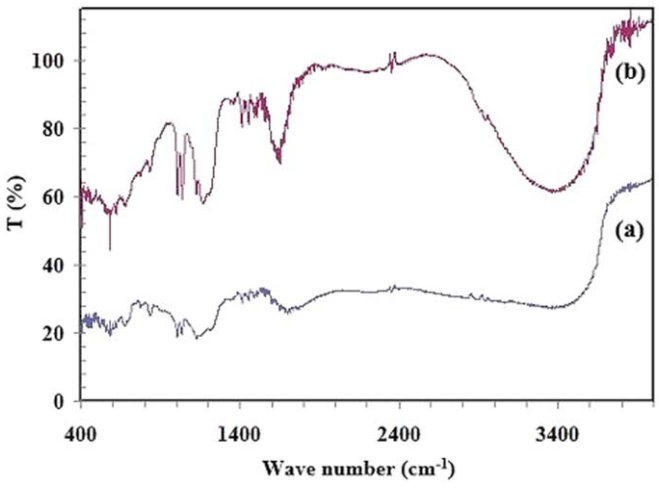

Figure 4. FT-IR spectra of Amberlyst–15: (a) before, and (b) after adsorption of Cd(II) at 303 K and pH 5.

pseudo-first order model can be given as:

$$\mathrm{In}(q_e - q_t) = \mathrm{In}\ \mathrm{q_e} - k_1 t \tag{3}$$

In equation (3), k_1 (m^{-1}) represents the rate constant for pseudo-first order while q_e and q_t are the amount of metal ions adsorbed (mol/g) at equilibrium and time *t* respectively. The q_e and k_1 values were determined from the intercept and slop respectively by linear plotting of $\ln(q_e - q_t)$ verses t (figure 6(a)). Similarly, linear form of pseudo-second order model is given by the equation as:

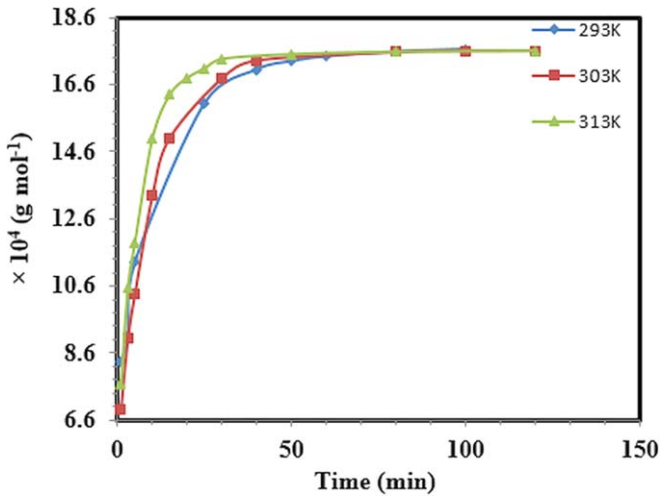

Figure 5. Effect of contact time on the adsorption of Cd(II) onto Amberlyst-15 at 303 K and pH 5.

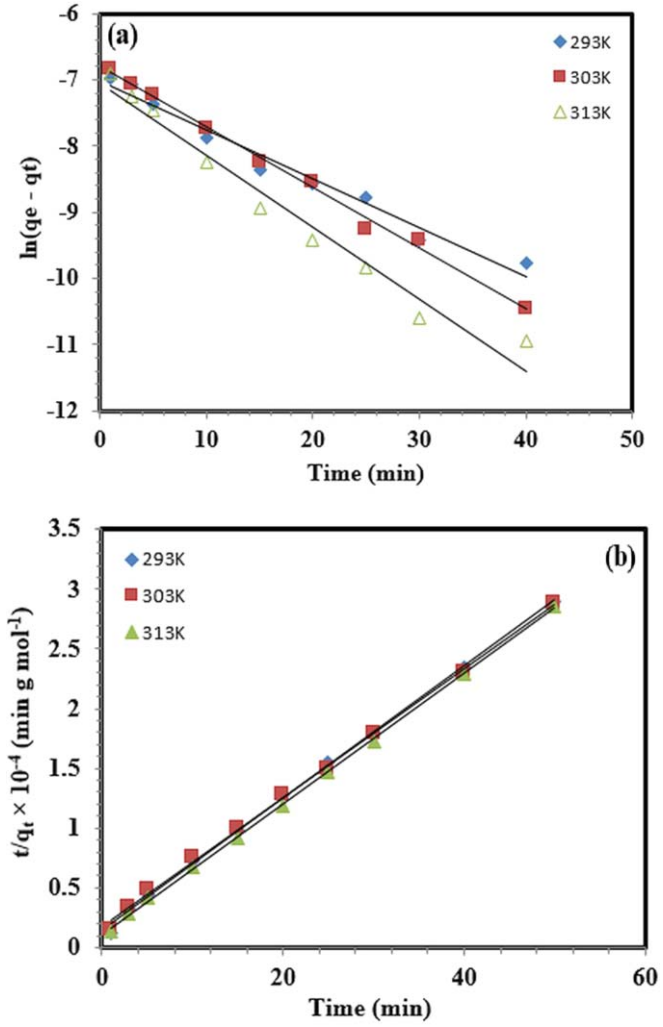

Figure 6. (a). Pseudo-first order plot for the adsorption of Cd(II) onto Amberlyst-15 at 303 K and pH 5, (b). Pseudo-second order plot for the adsorption of Cd(II) onto Amberlyst-15 at 303 K and pH 5.

$$\frac{t}{q_t} = \frac{1}{k_2 {q_e}^2} + \frac{t}{q_e} \tag{4}$$

Table 1. Kinetic parameters for Cd(II) adsorption onto Amberlyst-15 at different temperature and pH 5.

	Temperature (K)		
Kinetic models	293	303	313
$q_{e,exp} \times 10^4$ (mol/g)	17.6	17.6	17.6
Pseudo-first-order			
k_1 (min^{-1})	0.06	0.07	0.09
$q_{e,cal} \times 10^4$ (mol/g)	8.4	8.7	7.5
R^2	0.990	0.977	0.954
Pseudo-second-order			
k_2 ($g \cdot mg^{-1} \cdot min^{-1}$)	333.7	341.7	547.3
$q_{e,cal} \times 10^4$ (mol/g)	17.6	17.6	17.6
R^2	0.999	0.999	1

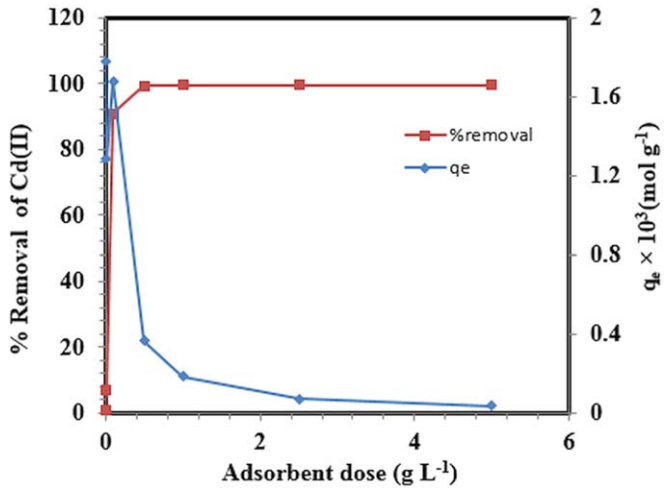

Figure 7. Effect of adsorbent dose on the adsorption of Cd(II) onto Amberlyst-15 at 303 KpH5.

In equation (4), k_2 represents the pseudo-second order rate constant (g/mg.min) while q_e and q_t are the amount of Cd(II) adsorbed at equilibrium and time *t*, respectively. The k_2 and q_e values were assessed from the intercept and slope respectively from linear plotting of t/q_t verses t (figure 6(b)).

The kinetic parameters obtained from both kinetic models are summarized in table 1. It is obvious from table that pseudo-first order model could not give satisfactory results due to low correlation coefficient (R^2) values and inconsistency of $q_{e.cal}$ with the q_{exp}. Conversely, the R^2 values obtained from pseudo-second order are very high, closer to linearity. Moreover, the q_e values calculated from pseudo-second order were in close agreement to the experimental values. Therefore, on the basis of above findings, conclusion can be made that pseudo-second order model describes better the adsorption of Cd(II) ions onto Amberlyst-15 [43].

3.2.3. Effect of adsorbent dosage

Amount of adsorbent plays an important role in the adsorption process by providing a greater number of active sites. The effect of adsorbent dose on Cd(II) adsorption is shown in figure 7 which shows that initially the adsorption rate was very fast and percentage removal of metal ions was increased sharply by increasing the adsorbent dosage. The percentage removal of Cd(II) was increased from 90.76 to 99.5% with increasing the Amberlyst.15 dosage from 0.1 to 5 g. On the other hand, the adsorption in mol per gram was observed to decrease. This behavior can be attributed to the fact that at higher adsorbent dosage the numbers of active sites available for the adsorption process are abundant and surface area of adsorbent is greater [44]. However, the percentage removal becomes almost constant when the adsorbent amount exceeds than 0.5 g. The decrease in total adsorption may be due to the un-occupation of binding sites available on the surface of adsorbent and deficiency of metal ions for more effective saturation of binding sites. Furthermore, at higher adsorbent dosage, solid particles can create electrostatic repulsions or block some active sites from adsorbate species which can possibly stop the attraction between absorbing species and active sites of adsorbent [45, 46].

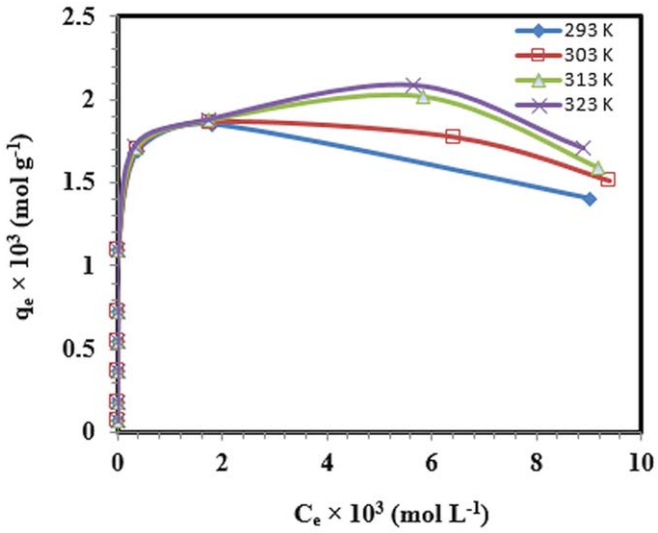

Figure 8. Effect of temperature on the adsorption of Cd(II) onto Amberlyst −15 at pH 5.

3.2.4. Effect of concentration

The adsorption isotherms at different temperatures (293–323 K) are presented in figure 8 which reflects the effect of concentration and temperature on adsorption of Cd(II) by Amberlyst-15. The adsorption capacity of Amberlyst-15 was observed to increase with increasing temperature and concentration of metal ion solution until an equilibrium is obtained which clearly implies the endothermic nature of ion exchange adsorption process.

The maximum adsorption capacity for Cd(II) adsorption was obtained 2.01 mmol g^{-1} at 323 K. The increased absorption capacity with increasing initial concentration may be due to the result of increasing driving force provided by concentration gradient responsible of effective collision between metal ions and adsorbent surface. The positive effect of temperature might be due to the fact that the mobility of Cd(II) ions was efficient and the number of binding sites on the Amberlyst.15 were increased at a higher temperature. The increase in temperature of the system can also results in enhancement of the thickness of boundary and hence an increase in adsorption. Moreover, an increase in temperature may also cause an enlargement in the pore diameter of the particles which results in an enhanced adsorption [47, 48].

3.2.5. Effect of pH

pH is one of the most important parameters which affects the dissociation of active sites as well as the hydrolysis, complexation, solution chemistry and precipitation of metal ions. The effect of pH on removal of Cd(II) onto Amberlyst−15 was investigated and results are illustrated in figure 9.

It can be predicted from the figure that adsorption was strongly controlled by the pH of the metal ion solution and resin have showed highly efficient adsorption potential even at highly acidic conditions. The maximum adsorption of Cd(II) was occurred at pH 3 which selected as optimum pH for further adsorption experiments. However, beyond pH 3, adsorption was observed to decrease from pH 4–7. This unusual behavior may be due to the replacement of H^+ ions from the sulfonate groups of the resin by metal hydroxyl ions [49]. Similarly, it was also assumed that at high pH, presence of OH^- ions in alkaline medium affect the $Cd(OH)^+$ hydrolysis as well as $Cd(OH)_2$ complexation and hence adsorption decreased due to precipitation formation. Several reactions can occur between adsorbing metal ions and the groups present on the surface of the adsorbent which can lead to the formation of some complexes, such as, ion-pair or coordinative surface complexes depending upon the interaction between the adsorbing metal ions and the surface-active groups. In case of Cd(II), the following reactions are expected to occur in aqueous media:

$$Cd^{2+} + H_2O \rightleftarrows Cd(OH)^+ + H^+ \quad (5)$$

As R-SO_3H can efficiently release its protons and thus we can write:

$$R - SO_3H + H_2O \rightleftarrows R - SO_3 + H^+ + H_3O^+(H^+ + H_2O) \quad (6)$$

Combination of equations (5) and (6)gives equation in the form:

$$R - SO_3H + Cd^{2+} + 2H_2O \rightleftarrows R - SO_3Cd^{2+}(OH)^+ + 2H^+ \quad (7)$$

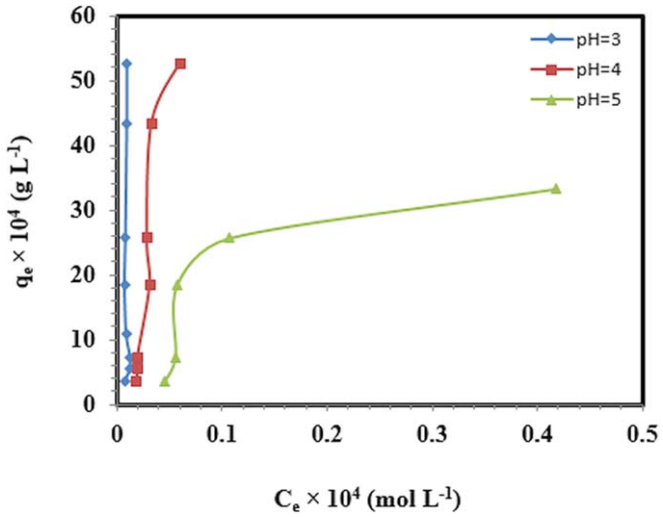

Figure 9. Effect of pH on the adsorption of Cd(II) onto Amberlyst-15 303 K.

It can be concluded from equation (7) that the recommended mechanism for the exchange of Cd(II) is coordinative and inner-sphere complexation [50].

3.3. Application of adsorption isotherm models

Adsorption isotherms are mathematical relationships which describe the distribution of adsorbate between aqueous and solid phases at a specific or constant temperature. The shapes of isotherms provide many assumptions regarding the nature of the adsorption, interaction among adsorbate and adsorbent, surface coverage and heterogeneity of the adsorbent surface [51]. Different adsorption isotherm models such as Langmuir, Freundlich and Dubinin-Radushkevitch in the present work were employed to evaluate the equilibrium data; however, the isotherm that yields higher regression values (R^2) and have a minimum deviation between the calculated and experimental adsorption capacities are discussed here. Langmuir model describes the monolayer adsorption on uniform surface of adsorbent due to the availability of finite number of adsorption sites. Accordingly, when a particular adsorption sites are filled then no further adsorption can take place at that sites and thus the surface of adsorbent is eventually reached at saturation value where maximum adsorption occurs. The Langmuir isotherm was applied in the present work to elucidate the adsorption of Cd(II) onto Amberlyst-15. The magnitudes of q_m and K_b were calculated from the slope and intercept of linear plots between C_e/q_e verses C_e, shown in figure 10, respectively by using the equation given below:

$$\frac{C_e}{q_e} = \frac{1}{k_b q_m} + \frac{C_e}{q_m} \tag{8}$$

where C_e, q_m and K_b represents the equilibrium concentration (mol/l), maximum adsorption capacity(mol/g) and binding energy constant (L/g), respectively. The Langmuir parameters are listed in table 2 which indicates that q_m and K_b increases with an increase in temperature. The enhancement in q_m with increasing temperature can be associated to the availability of more active sites, whereas an increase in K_b values points that metal ions are more firmly adsorbed on the surface of resin [52]. Moreover, an important dimensionless parameter (R_L) was utilized to judge the favorability of metal ion adsorption on the resin from equation:

$$R_L = \frac{1}{1 + k_b + C_o} \tag{9}$$

In equation (9), C_o and K_b represents the initial metal ions concentration (mol/L) and Langmuir constant, respectively. The R_L values were also calculated by using equation (9) which lies in the range of 0.001–0.005 (table 2), suggesting the favorable nature of adsorption process. To predict the nature of adsorption either it is physical, chemical or simply ion exchange, adsorption free energy (E) was determined with the help of D-R model given below:

$$\ln q_e = \ln q_m + \beta\varepsilon^2 \tag{10}$$

where q_e and q_m represents the theoretical adsorption capacity and maximum adsorption capacity, respectively, β is related to mean energy of sorption (E) and ε is the Polanyi potential associated with maximum adsorption capacity which can be described in the from:

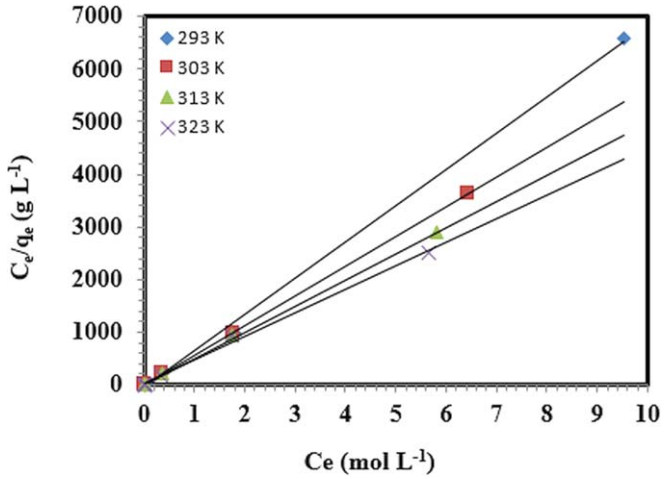

Figure 10. Langmuir plot for the adsorption of Cd(II) onto Amberlyst-15 at different temperatures and pH 5.

Table 2. The parameters of Langmuir and Dubinin-Radushkevich isotherms for the adsorption of Cd(II) onto Amberlyst-15 at pH 5.

		Temperature (K)			
Adsorption model	Parameter	293	303	313	323
Langmuir	$q_{m,\,exp} \times 10^3$ (mol/g)	1.85	186	1.87	1.88
	$q_{m,\,calc} \times 10^3$ (mol/g)	1.45	1.51	1.84	2.01
	K_b (L/g)	66417	119177	136751	156441
	R_L	0.005	0.004	0.002	0.001
	R^2	0.99	0.99	0.99	0.99
Dubinin-Radushkevich	$q_{m,\,calc} \times 10^3$ (mol/g)	2.36	3.22	3.78	4.58
	β (mol^2 kJ^{-2})	0.0026	0.0028	0.0022	0.0025
	E (kJ mol^{-1})	13.8	13.36	15	14
	R^2	0.82	0.95	0.92	0.99

$$\varepsilon = \mathrm{RTln}\left(1 + \frac{1}{C_e}\right) \tag{11}$$

where R, T and C_e represents general gas constant (J.mol^{-1}.k^{-1}), absolute temperature (K) and metal ion concentration(mol l^{-1}), respectively. The q_e versus ε^2 linear plots at different temperatures are mentioned in figure 11 where the intercepts and slopes of the plots were used to calculate the q_m and β values listed in table 2. Similarly, the equation (12) was used to calculate mean free energy value as:

$$\mathrm{E} = \frac{1}{(2\beta)^{1/2}} \tag{12}$$

When the values of E are less than 8 kJ mol^{-1} indicate the physical adsorption and greater than 16 kJ mol^{-1} represents chemical adsorption while in the range 8–16 kJ mol^{-1} ion exchange removal mechanism [5]. It is clear from the table 2 that E values (13–15 kJ mol^{-1}) for all the temperatures obtained from the above equation resides in the range 8–16 kJ mol^{-1} which confirms the ion exchange reaction mechanism of Cd(II) removal onto Amberlyst-15. A small deviation between the experimental and calculated q_m values may be due to the basic mathematical principles which are involved in the formulation of this model and shape of the isotherm.

3.4. Thermodynamic evaluation

In the present investigations, different thermodynamic parameters such as Gibbs free energy (ΔG), enthalpy change (ΔH) and entropy change (ΔS) were determined using equations (13) and (14) given as

$$(\Delta G) = -RT \ln K_b \tag{13}$$

$$\ln K_b = -\frac{(\Delta H)}{RT} + \frac{\Delta S}{R} \tag{14}$$

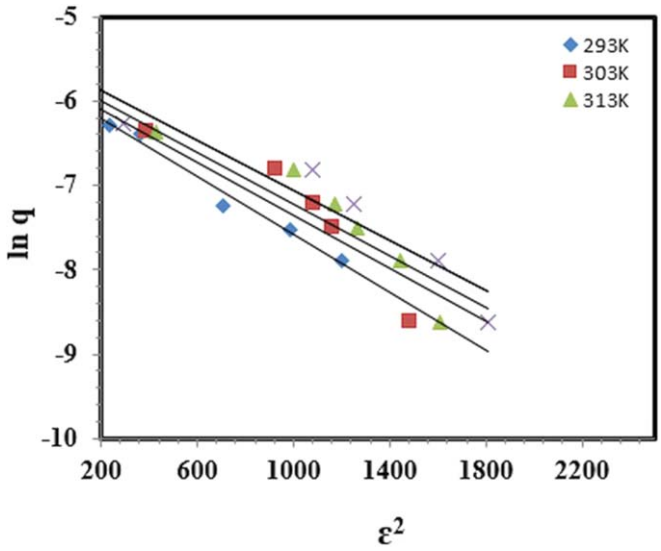

Figure 11. D-R plots for the adsorption of Cd(II) onto Amberlyst-15 at different temperatures and pH 5.

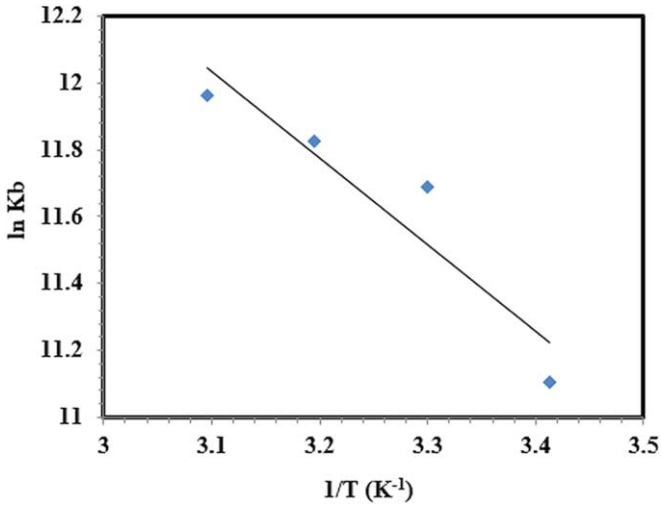

Figure 12. Vant't Hoff plot for the adsorption of Cd(II) onto Amberlyst-15 at pH 5.

Table 3. Thermodynamic parameters for the desorption of Cd(II) onto Amberlyst-15 at pH 5.

Temperature (K)	ΔG (kJ mol^{-1})	ΔH (kJ mol^{-1})	ΔS (J mol^{-1} K^{-1})
293	−27.35		
303	−29.01	21.52	166.78
313	−30.68		
323	−32.35		

The ΔH and ΔS values were computed from the slope and intercept of linear plots of lnK_b verses 1/T as mentioned in figure 12 and thermodynamic parameters are tabulated in table 3. The ΔG values are observed to increase from −27 to −32 kJ mol^{-1} with the rise in temperature from 293 to 323 K indicating the exchange reaction was spontaneous and feasible in nature. The positive value of ΔH suggested the endothermic nature of adsorption process whereas the positive value of ΔS refers the randomness at the solid solution interface.

Table 4. Comparison of maximum adsorption capacities (mmol/g) of Cd(III) by various synthetic resins.

Ion exchange resins	Maximum adsorption capacity Xm (mmol/g)	References
Duolite ES 467	0.123	[53]
C 160	0.282	[54]
Lewatit Mono Plus SP112	0.313	[55]
Amberlite 200 C	0.351	
MCER	0.418	[56]
CEPR	0.418	
Dowex 50 W	0.246	[57]
Lewatit TP260	0.684	[58]
Duolite GT-73	0.943	[59]
Amberjet 1200 H	1.5	[60]
Amberlite.IR-120	1.65	[61]
Amberlyst.15	2.01	**Present Study**

3.5. Comparison of amberlyst.15 performance

The monolayer adsorption capacity of Amberlyst.15 obtained in this work was compared with previously published results for Cd(II) adsorption by using different commercially available synthetic cation exchange resins. The comparative analysis given in table 4 has proved that maximum adsorption capacity of Amberlyst.15 was higher than those of other reported resins. This also confirmed that Amberlyst.15 has a greatest adsorption potential due to large surface area and porous structure and thus could be used as a promising adsorbent for Cd(II) removal from aqueous solutions.

4. Conclusions

The present investigation demonstrated that Amberlyst-15 can be used as an efficient and potential adsorbent for removal of Cd (II) from the aqueous solutions at domestic and pilot scale. SEM-EDS, FT-IR, TGA and BET analysis revealed that Amberlyst-15 has an amorphous and highly porous structure and also confirmed the successful exchange of Cd(II) on the surface of resin. Furthermore, Amberlyst 15 showed features of high adsorption capacity and fast kinetics for removing Cd(II). According to our optimization, Amberlyst 15 can remove 99.95% of Cd(II) in 30 min equilibrium time at temperature of 323 K, pH 3, stirring rate 120 rpm with dosage of the resin 0.5 g. The maximum monolayer adsorption capacity (2.01 mmol g^{-1}) of resin used in the present investigation was comparable to the reported one in literature for Cd(II) adsorption on different commercially available ion exchange resins. Expressing such high removal efficiency and convenient operation, Amberlyst.15 can be implemented as a novel and potential adsorbent for the removal of Cd(II) in water and waste water treatment systems.

Acknowledgments

Authors are thankful for the financial support provided by Higher Education Commission of Pakistan under National Research Program for Universities (NRPU), Project No. 8817.

ORCID iDs

Muhammad Fahad https://orcid.org/0000-0002-0683-0991

References

[1] Naushad M, Sharma G and Zeid A A 2019 Photodegradation of toxic dye using Gum Arabic-crosslinkedpoly(acrylamide)/Ni(OH)$_2$/FeOOH nanocomposites hydrogel *J. Clean. Prod.* **241** 118263

[2] Naushad M, Alothman Z A, Awual M R, Alam M M and Eldesoky G E 2015 Adsorption kinetics, isotherms, and thermodynamic studies for the adsorption of Pb^{2+} and Hg^{2+} metal ions from aqueous medium using Ti(IV) iodovanadate cation exchanger *Ionics* **21** 2237–45

[3] Naushad M 2014 Surfactant assisted nano-composite cation exchanger: Development, characterization and applications for the removal of toxic Pb2 + from aqueous medium *Chem. Eng. J.* **235** 100–8

[4] Alothman Z A, Inamuddin and Naushad M 2013 Recent developments in the synthesis, characterization and applications of zirconium (IV) based composite ion exchangers *J. Inorg. Organomet. Polym.* **23** 257–69
[5] Mironyuk I, Tatarchuk T, Naushad M, Vasylyeva H and Mykytyn I 2019 Highly efficient adsorption of strontium ions by carbonated mesoporous TiO_2 *J. Mol. Liq.* **285** 742–53
[6] Shah K H, Ayub M, Fahad M, Bilal M, Amin B A Z and Hussain Z 2019 Natural dolomite as a low-cost adsorbent for efficient removal of As(III) from aqueous solutions *Mater. Res. Express* **6** 085535
[7] Mittal A, Naushad M, Sharma G, Alothman Z A, Wabaidur S M and Alam M 2016 Fabrication of MWCNTs/ThO_2 nanocomposite and its adsorption behavior for the removal of Pb(II) metal from aqueous medium *Desalin. Water Treat.* **57** 21863–9
[8] Naushad M, Vasudevan S, Sharma G, Kumar A and Zeid A A 2016 Adsorption kinetics, isotherms, and thermodynamic studies for Hg^{2+} adsorption from aqueous medium using alizarin red-S-loaded amberlite IRA-400 resin *Desalin. Water Treat.* **57** 18551–9
[9] Naushad M and Zeid A A 2015 Separation of toxic Pb^{2+} metal from aqueous solution using strongly acidic cation-exchange resin: analytical applications for the removal of metal ions from pharmaceutical formulation *Desalin. Water Treat.* **53** 2158–66
[10] Naushad M, Mittal A, Rathorec M and Gupta V 2015 Ion-exchange kinetic studies for Cd(II), Co(II), Cu(II), and Pb(II) metal ions over a composite cation exchanger *Desalin. Water Treat.* **54** 2883–90
[11] Gupta V K and Rastogi A 2008 Equilibrium and kinetic modeling of cadmium(II) biosorption by non-living algal biomass Oedogonium sp. from aqueous phase *J. Hazard. Mater.* **153** 759–66
[12] Gupta V K and Rastogi A 2008 Biosorption of lead from aqueous solutions by green algae spirogyra species: kinetics and equilibrium studies *J. Hazard. Mater.* **152** 407–14
[13] Zhao Q, Gao Y and Ye Z 2013 Reduction of COD in TNT Red water through adsorption on macroporous polystyrene resin RS 50B *Vacuum* **95** 71–5
[14] Zhao Z, Zhang J, Chena X, Liua X, Li J and Zhang W 2013 Separation of tungsten and molybdenum using macroporous resin: Equilibrium adsorption for single and binary systems *Hydrometallurgy* **140** 120–7
[15] Rengaraj S, Yeon K H, Kang S Y, Lee J U, Kim K W and Moon S H 2002 Studies on adsorptive removal of Co(II), Cr(III) and Ni(II) by IRN77 cation-exchange resin *J. Hazard. Mater.* **92** 185–98
[16] Dizge N, Keskinler B and Barlas H 2009 Sorption of Ni(II) ions from aqueous solution by Lewatit cation-exchange resin *J. Hazard. Mater.* **167** 915–26
[17] Xiong C, Yu-jie F and Caiping Y 2009 Adsorption of Pb(II) on macroporous weak acid adsorbent resin from aqueous solutions: batch and column studies *J. Cent. South Univ. Technol.* **16** 569–74
[18] Xiong C, Yu-jie F, Caiping Y and Chen S 2010 Removal of Co(II) from aqueous solutions by NKC-9 strong acid resin *Trans. Nonferrous Met. Soc. China* **20** 1141–7
[19] Xiong C and Yao C 2011 Ion exchange recovery of Ni(II) on macroporous weak acid resin (D151 resin) *Indian J. Chem. Technol.* **18** 13–20
[20] Xiong C, Jingfei Z, Chen S and Qing C 2012 Adsorption and desorption of praseodymium (III) from aqueous Solution using D72 Resin *Chinese J. Chem. Eng.* **20** 823–30
[21] Xiong C 2008 Sorption Behaviour of D155 resin for Ce(III) *Indian J. Chem.* **47A** 1377–80
[22] Xiong C 2008 Study on sorption of D155 resin for gadolinium *J. Rare Earth* **26** 258–63
[23] Alguacil F J, Diaz I G and Lopez F 2012 The removal of chromium (III) from aqueous solution by ion exchange on Amberlite 200 resin: batch and continuous ion exchange modeling *Desalin. Water Treat.* **45** 55–60
[24] Sahu S K, Meshram P, Pandey B D, Kumar V and Mankh T R 2009 Removal of chromium(III) by cation exchange resin, Indion 790 for tannery waste treatment *Hydrometallurgy* **99** 170–4
[25] Talukder M M R, Wu J C, Lau S K, Cui L C, Shimin G and Lim A 2009 Comparison of Novozym 435 and amberlyst 15 as heterogeneous catalyst for production of biodiesel from palm fatty acid distillate *Energy Fuels* **23** 1–4
[26] Shah K h, Mustafa S, Waseem M, Hamayun M, Shah F, Rehman W and Khan A R 2017 Competitive exchange of Cr (III) sorption on macroporous Amberlyst.15 (H) *Mater. Res. Express* **4** 015502
[27] Kula I, Ugurlu M, Karaoglu H and Celik A 2008 Adsorption of Cd(II) ions aqueous solutions using activated carbon prepared from olive stone by $ZnCl_2$ activation *Bioresour. Technol.* **99** 492–501
[28] Wang Y, Tang X, Chen Y, Zhan L, Li Z and Tang Q 2009 Adsorption behavior and mechanism of Cd(II) on loess soil from China *J. Hazard. Mater.* **172** 30–7
[29] Shah K H, Ali S, Shah F, Waseem M, Ismail B, Khan R A, Khan A M and Khan A R 2018 Magnetic oxide nanoparticles (Fe3O4) impregnated bentonite clay as a potential adsorbent for Cr(III) *adsorption Mater. Res. Express* **5** 096102
[30] Pal A, Pan S and Saha S 2013 Synergistically improved adsorption of anionic surfactants and crystal violet on chistosan hydrogel beads *Chem. Eng. J.* **217** 426–34
[31] Han Y G, Kusunose T and Sekino T 2009 One-step reverse micelle polymerization of organic dispersible polyaniline nanoparticles *Synth. Met.* **159** 123–31
[32] Sheela T, Nayaka Y A, Vishwanatha R, Basavanna S and Venkatesha T G 2012 Kinetic and thermodynamic studies on the adsorption of Zn(II), Cd(II) and Hg(II) from aqueous solution using zinc oxide nanoparticles *Powder Technol.* **217** 163–70
[33] Mahmood T, Saddique M T, Naeem A, Mustafa S, Dilara B and Raza Z A 2011 Cationic exchange removal of Cd^{2+} from aqueous solution by NiO *J. Hazard. Mater.* **185** 824–8
[34] Alyuz B and Veli S 2009 Kinetics and equilibrium studies for the removal of nickel and zinc from aqueous solutions by ion exchange resins *J. Hazard. Mater.* **167** 482–8
[35] Paola A D, Marci G, Schiavello M, Uosaki K, Ikeda S and Ohtani B 2002 Preparation of polycrystalline TiO_2photocatylyst impregnated with various transition metal ions: Characterization and photocatalytic activity for the degradation of 4-nitrophenol *J. Phys. Chem. B* **106** 637–45
[36] Malkoc E and Nuhoglu Y 2006 Removal of Ni(II) ions from aqueous solutions using waste oftea factory: Adsorption on a fixed-bed column *J. Hazard. Mater.* **135** 328–36
[37] Reddy D H K, Ramana D K V, Seshaiah K and Reddy A V R 2011 Biosorption of Ni(II) from aqueous phase by Moringaoleifra bark, a low cost biosorbent *Desalination* **268** 150–7
[38] Prasad M N V, Lalharuaitluanga H and Radha K 2011 Potential of chemically activated and raw charcoals of Melocannabaccifera for removal of Ni(II) and Zn(II) from aqueous solutions *Desalination* **271** 301–8
[39] Argun M E, Dursun S, Ozdemir C and Kartas M 2007 Heavy metal adsorption by modified sawdust. Thermodynamics and kinetics *J. Hazard. Mater.* **141** 77–85
[40] Naiya T K, Bhattacharya A K and Das S K 2009 Adsorption of Cd(II) and Pb(II) from aqueous solutions on activated alumina *J. Colloid Interf. Sci.* **333** 14–26

[41] Jain C K and Sharma M K 2002 Adsorption of cadmium on bed sediments of river Hindon: Adsorption models and kinetics *Water Air Soil Pollut.* **137** 1–19
[42] Zhang L, Liu N, Yang L and Lin Q 2009 Sorption behavior of nano-TiO_2 for the removal of selenium ions from aqueous solution *J. Hazard. Mater.* **170** 1197–203
[43] Fil B A, Yilmaz A E, Boncukcuoglu R and Bayar S 2012 Removal of divalent heavy metal ions from aqueous solutions by Dowex HCR-S synthetic resin *Bulgar. Chem. Comm.* **44** 201–7
[44] Phuengprasop T, Sittiwong J and Unob F 2011 Removal of heavy metal ions by iron oxide coated sewage sludge *J. Hazard. Mater.* **186** 502–7
[45] Sen T K and Sarzali M V 2008 Removal of cadmium metal ion (Cd^{2+}) from its aqueous solution by aluminum oxide (Al_2O_3): A kinetic and equilibrium study *Chem. Eng. J.* **142** 256–62
[46] Erdem M and Ozverdi A 2006 Kinetics and thermodynamics of Cd(II) adsorption onto pyrite and synthetic iron sulphide *Sep. Purif. Technol.* **51** 240–6
[47] Bugariu L, Ratoi M, Bulgariu D and Macoveanu M 2008 Equilibrium study of Pb(II) and Hg(II) sorption from aqueous solutions by moss peat *Environ. Eng. Manag. J.* **7** 511–6
[48] Namasivayam C and Ranganathan K 1995 Removal of Cd(II) from wastewater by adsorption on 'Waste' *Fe(III)/Cr(III) hydroxide Water Res.* **29** 1737–44
[49] Erlvgay N and Bayhan Y K 2010 Removal of Cu(II) ions using mushroom biomass (Agaricusbisporus) and kinetic modeling *Desalination* **255** 137–42
[50] Vohra M S and Davis A P 1997 Adsorption of Pb(II), NTA, and Pb-NTA onto TiO_2 *J. Colloid Interf. Sci.* **194** 59–67
[51] Faisal A A H, Al-Wakelb S F A, Assib H A, Najia L A and Naushad M 2020 Waterworks sludge-filter sand permeable reactive barrier for removal of toxic lead ions from contaminated groundwater *J. Water Process Eng.* **33** 101112
[52] Waseem M, Mustafa S, Naeem A, Shah K H, Samad S Y and Safdar M 2010 Modeling of Cd (II) sorption on mixed oxide *J. Chem. Soc. Pak.* **33** 619–23
[53] Rao K S, Chaudhury G R and Mishra B K 2010 Kinetics and equilibrium studies for the removal of cadmium ions from aqueous solutions using Duolite ES 467 resin *Int. J. Miner. Process.* **97** 68–73
[54] Bożęcka A, Orlof-naturalna M and Sanak-Rydlewska S 2016 Removal of lead, cadmium and copper ions from aqueous solutions by using ion exchange resin C 160 *Miner. Resourc. Manag.* **32** 129–40
[55] Otrembska P and Gega J 2013 Kinetic studies on sorption of Ni(II) and Cd(II) from chloride solutions using selected acidic cation exchangers *Physicochem. Probl. Miner. Process.* **49** 301–12
[56] Wang Z, Ding S, Li Z, Li F, Zhao T, Li J, Lin H and Chen C 2018 Synthesis of a magnetic polystyrene-based cation exchange resin and its utilization for the efficient removal of cadmium (II) *Water Sci. Technol.* **2017** 770–81
[57] Pehlivan E and Altun T 2006 The study of various parameters affecting the ion exchange ofCu^{2+},Zn^{2+},Ni^{2+},Cd^{2+}, and $Pb^{2+}$from aqueous solution on Dowex 50W synthetic resin *J. Hazard. Mat. B* **134** 149–56
[58] Alguacil F J 2003 A kinetic study of cadmium(II) adsorption on Lewatit TP260 resin *J. Chem. Res.* **3** 144–6
[59] Bhatt R R, Shah B and Shah A V 2012 Uptake of heavy metal ions by chelating ion-exchange resin derived from p-hydroxybenzoic acid-formaldehyde-resorcinol: Synthesis, characterization and sorptiondynamics *MJAS* **16** 117–33
[60] Bai Y and Bartkiewicz B 2009 Removal of cadmium from wastewater using ion exchange resin amberjet 1200H columns *Polish J. of Environ. Stud.* **18** 1191–5
[61] Demirbas P E, Gode F, Altun T and Arslan G 2005 Adsorption of Cu(II), Zn(II), Ni(II), Pb(II), and Cd(II) from aqueous solution on Amberlite IR-120 synthetic resin *J. Colloid Interface Sci.* **282** 20–5